JOURNAL OF GEOPHYSICAL RESEARCH, VOL. 104, NO. D15, PAGES 18,755-18,768, AUGUST 20, 1999

A test of our understanding of the ozone chemistry in the Arctic polar vortex based on in situ measurements of ClO, BrO, and O_3 in the 1994/1995 winter

Thomas Woyke,[1] Rolf Müller,[1] Fred Stroh,[1] Daniel S. McKenna,[1]
Andreas Engel,[2] James J. Margitan,[3] Markus Rex,[3,4] and
Kenneth S. Carslaw[5,6]

Abstract. We present an analysis of in situ measurements of ClO, BrO, O_3, and long-lived tracers obtained on a balloon flight in the Arctic polar vortex launched from Kiruna, Sweden, 68°N, on February 3, 1995. Using the method of tracer correlations, we deduce that the air masses sampled at an altitude of 21 km (480 K potential temperature), where a layer of enhanced ClO mixing ratios of up to 1150 parts per trillion by volume was observed, experienced a cumulative chemical ozone loss of 1.0±0.3 ppmv between late November 1994 and early February 1995. This estimate of chemical ozone loss can be confirmed using independent data sets and independent methods. Calculations using a trajectory box model show that the simulations underestimate the cumulative ozone loss by approximately a factor of 2, although observed ClO and BrO mixing ratios are well reproduced by the model. Employing additional simulations of ozone loss rates for idealized conditions, we conclude that the known chlorine and bromine catalytic cycles destroying odd oxygen with the known rate constants and absorption cross sections do not quantitatively account for the early winter ozone losses infered for air masses observed at 21 km.

1. Introduction

Large-scale seasonal stratospheric ozone depletion was first observed over Antarctica [*Farman et al.*, 1985]. It is currently accepted [e.g., *Anderson et al.*, 1991; *Solomon et al.*, 1990; *World Meteorological Organization*, 1994] that the observed polar ozone loss is mainly due to chlorine and bromine radicals involved in catalytic cycles. At high concentrations of chlorine radicals the ClO dimer cycle [*Molina et al.*, 1987] and the BrO-ClO cycle [*McElroy et al.*, 1986] provide efficient ozone destruction mechanisms. High ClO concentrations are typical for Antarctic polar vortex conditions and are ultimately caused by the release of active chlorine species from the chlorine reservoir species HCl and $ClONO_2$ by heterogeneous reactions on polar stratospheric clouds (PSCs), which form at low temperatures (typically below 195 K) inside the vortex.

The observation of enhanced ClO-mixing ratios [*Brune et al.*, 1990; *Waters et al.*, 1993] in the Arctic polar vortex has shown that processes similar to those observed over Antarctica also occur in the Northern Hemisphere. The Arctic polar vortex exhibits a greater dynamical activity, which introduces a large variability into ozone measurements. Thus determining chemical ozone loss becomes a difficult task. Two complementary types of approaches have recently been employed to estimate Arctic polar ozone loss. The first one is based on the idea that given observations of halogen oxides a photochemical model can be used to compute ozone loss rates and thereby estimate chemical ozone loss [*McKenna et al.*, 1990; *Salawitch et al.*, 1990, 1993; *Brune et al.*, 1991]. Ozone loss rates derived in this way are of the order of 1% per day, thus it was concluded significant ozone depletion occurs in the Arctic polar vortex. The second type of approach is based on the comparison of ozone observations with an estimate of the amount of ozone that should be observed in the absence of chemical ozone loss. This estimate of non depleted ozone abundances can be achieved in several ways. The Match technique [*von der Gathen et al.*, 1995; *Rex et al.*, 1999] is based on the idea that ozone measurements at different times and locations can be linked by trajectory calculations: If a trajectory originating along the path of an ozone sonde A intersects the path of an later ozone sonde B, both measurements are as-

[1] Institut für Stratosphärische Chemie, Forschungszentrum Jülich, Jülich, Germany.
[2] Institut für Meteorologie und Geophysik, J.W. Goethe Universität Frankfurt, Frankfurt, Germany.
[3] Jet Propulsion Laboratory, Pasadena, California.
[4] Alfred Wegener Institute for Polar and Marine Research, Potsdam, Germany.
[5] MPI für Chemie, Mainz, Germany.
[6] Now at: Environment Centre, University of Leeds, Leeds, England, United Kingdom.

Paper number 1999JD900287.
0148-0227/99/1999JD900287$09.00

sumed to take place within the same air parcel. The estimate of chemical ozone loss for this air parcel is then given by the difference $O_3(B) - O_3(A)$. Given a large set of ozone soundings, the Match technique can be used to derive ozone loss rates, which can be integrated to provide information on cumulative ozone loss. Alternatively, transport calculations advecting a passive ozone tracer, either using a three-dimensional (3-D) model [*Hansen et al.*, 1997; *Goutail et al.*, 1999; *Deniel et al.*, 1998] or a reverse trajectory procedure [*Manney et al.*, 1996], are used to provide a reference to compare ozone measurements. This technique implicitly assumes a correct representation of transport processes in the model, which was checked by considering observed tracer fields [*Goutail et al.*, 1999; *Lefèvre et al.*, 1998]. Another powerful tool is the use of tracer correlations: empirically derived correlations between sufficiently long-lived species, valid for early winter before processing has occurred, provide a reference to compare the chemical composition of the sampled air masses at a later stage. This technique was first used to infer denitrification [*Fahey et al.*, 1990] and dehydration [*Kelly et al.*, 1989] in the Antarctic polar vortex and later applied to quantify Arctic polar ozone loss [*Proffitt et al.*, 1990, 1993; *Müller et al.*,1996, 1997]. These methods based on ozone observations have indeed shown a clear signature of chemical ozone loss in the Arctic in recent years, which is of the order of 20-50 % column ozone loss over the winter and early spring varying from year to year.

However, only a few comparisons of simulated ozone losses with derived ozone losses were made. *Hansen et al.* [1997], *Goutail et al.* [1999], and *Deniel et al.* [1998] find that the simulated ozone loss is less than the derived ozone loss in the 3-D model. But the measurements used there to infer the ozone loss lack simultaneous observations of the halogen oxides in the same air mass, so that the model is not well constrained. The other studies quoted, where ozone observations were used to infer chemical ozone loss, likewise lack observations of halogen oxides. Conversely, the studies quoted using observations of halogen radicals to estimate chemical ozone loss rates lack independent evidence of chemical ozone loss. Here we combine both: a measurement of halogen oxides inside the polar vortex and the ability to quantify chemical ozone loss for the same air masses independent of the halogen oxide measurement.

In the framework of the Second European Arctic and Midlatitude Experiment (SESAME) simultaneous observations of ClO, BrO, O_3, and of long-lived tracers were made on February 3, 1995. From this data set we derive an estimate of cumulative chemical ozone loss using the method of tracer correlations. This estimate of chemical ozone loss is verified using other independent data sets and methods. We present a model study addressing the question, whether the simulated cumulative ozone loss is consistent with the derived cumulative ozone loss. A sensitivity study of the simulation results is presented. We then discuss our results with regard to ozone loss rates derived by the Match technique. This study indicates that the simulations severely underestimate the cumulative ozone loss derived from observations.

2. Observations

This study is based on in situ data obtained on February 3, 1995, with a balloon-borne payload consisting of a cryogenic whole air sampler, an ozone photometer and a ClO/BrO instrument. The balloon was launched from Kiruna, Sweden (68°N, 21°E), at 0600 UT, reached its ceiling altitude of 17 hPa (≈28 km) at around 0830 UT and descended slowly to 23 km. Below 23 km, measurements were made during a fast parachute descent that took place near 64°N/25°E. Based on the Potential Vorticity (PV) analysis, measurements were made inside the Arctic polar vortex.

The cryogenic whole air sampler [*Schmidt et al.*, 1987] consists of 15 liquid neon cooled evacuated sample flasks, which are filled with ambient air during the flight. The samples are subsequently analyzed in the laboratory employing gas chromatographic techniques. Species analyzed are long-lived tracers such as CH_4, N_2O, and several chlorofluorocarbons, which represent 95% of the chlorine-containing source gases. From the measured chlorinated organics it is possible to determine the amount of total available chlorine Cl_y [*Schmidt et al.*, 1994; *Engel et al.*, 1997]. The accuracy of the measurements is better than 5%. The ClO-BrO instrument is based on the well-established chemical conversion resonance fluorescence technique [*Brune et al.*, 1989; *Toohey et al.*, 1993]; it has an accuracy of 20% for ClO and 30% for BrO with a detection limit of about 5 parts per trillion by volume (pptv) for one 20 s measurement cycle. The dual cell ozone photometer [*Proffitt and McLaughlin*, 1983] employs an UV absorption technique with an accuracy estimated to be better than 5% and a time resolution of 1 s.

Observations are shown in Figure 1. The main feature is a layer of enhanced ClO mixing ratios of up to 1150 pptv between 450 and 550 K potential temperature (19 to 23 km) coinciding with a local minimum in ozone with mixing ratios as low as 2.4 ppmv. BrO mixing ratios are about 10 pptv at these altitudes. The results of the halogen oxide measurements have been discussed elsewhere [*McKinney et al.*, 1997; *Pierson et al.*, 1999]. Here we focus on the analysis of ozone loss processes.

3. Deriving the Ozone Loss

3.1. Analysis of the in Situ Data of February 3, 1995

The anti correlation between O_3 and ClO mixing ratios between 450 and 550 K suggests that the local minimum in ozone mixing ratios is due to chemical ozone loss processes. To verify this hypothesis, we employ the technique of tracer correlations, which was shown by *Proffitt et al.* [1992] to be applicable to the problem of identifying chemical ozone loss in the polar vortex. Using a 2-D model, they have shown the existence of a compact correlation between N_2O and O_3 for the unperturbed Arctic polar vortex, since in the wintertime polar regions the photochemical lifetime of O_3 is sufficiently long, if chlorine activation on polar stratospheric clouds does not occur. Fast chemical ozone loss processes, for exam-

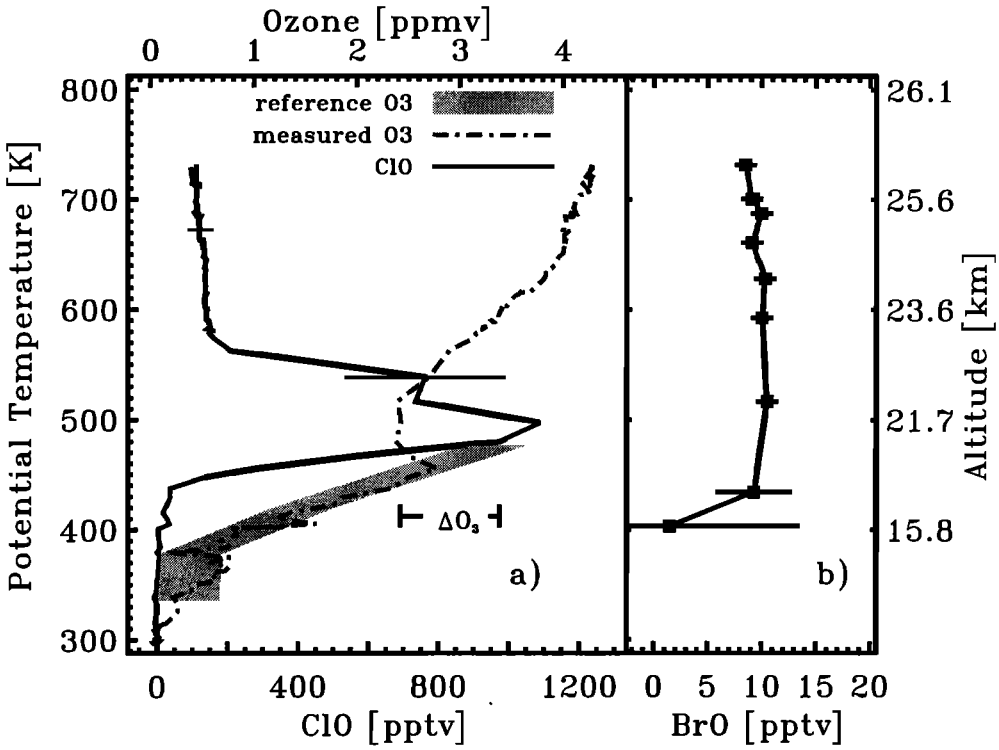

Figure 1. (a) O_3 and ClO mixing ratios as observed during the balloon descent on February 3, 1995. Error bars denote the 20% accuracy of the ClO measurement. Also shown is the calculated reference ozone mixing ratio $\hat{O}_3$ (see text). (b) Simultaneously observed BrO mixing ratio. Error bars denote the 1σ statistical precision of the BrO observations.

ple induced by chlorine activation, can then be identified by comparing the chemical composition of the sampled air masses with the one represented by the reference correlation valid for unperturbed conditions.

As a reference for our analysis, we use an update of the empirical correlation between CH_4 and O_3 mixing ratios derived by *Müller et al.* [1996] from observations made by the Halogen Occultation Experiment (HALOE) in the Arctic polar vortex in November 1994. The updated correlation (using V18 instead of V17 data) can be expressed as $O_3 = 5.08 \times CH_4{}^3 - 17.31 \times CH_4{}^2 + 14.61 \times CH_4 + 0.60$ (O_3 and CH_4 in ppmv, valid for $CH_4 = 0.5 - 1.6$ ppmv). The 1σ error of the calculated O_3 is 0.25 ppmv. The updated HALOE data set (V18) and the new correlation derived are shown in Figure 2. Using CH_4 instead of N_2O is dictated by the lack of simultaneous observations of N_2O and O_3 for the early winter 1994/1995 and is justified by noting that the photochemical lifetime of CH_4 in the polar vortices is also sufficiently long to expect a compact correlation with O_3. Since the temperatures in the polar vortex first fell below PSC existence temperatures in December 1994 [*Naujokat and Pawson*, 1996] these HALOE measurements can be considered representative for conditions inside the unperturbed Arctic polar vortex before the onset of chemical ozone loss. Thus the methane mixing ratio measured during the balloon flight can be used to calculate a proxy ozone mixing ratio $\hat{O}_3$ that would have been observed in the absence of any chemical ozone loss and if no mixing takes place across the vortex edge. The calculated $\hat{O}_3$ is also shown in Figure 1 as a grey shaded area.

At potential temperature levels between 300 and 450 K (10-19 km) the calculated $\hat{O}_3$ is mostly in agreement with the observed ozone mixing ratio, except between 350 and 380 K (12.5-14 km). Both the layered structure of the ozone profile and the meteorological analysis, showing that between 350 and 380 K the measurement location was closer to the vortex edge, suggest that mixing processes may have occurred there. Above 480 K (21 km) the observed methane mixing ratio of about 0.3 ppmv is below the lower limit of validity (0.6 ppmv) of the empirical correlation, so that no estimate of ozone loss can be given there. In the region of enhanced ClO mixing ratios at about 480 K the ozone measurements show 1.0 ± 0.3 ppmv (1σ) or ~ 30 % less than the calculated proxy ozone mixing ratio $\hat{O}_3$, which we consider to be chemical loss of ozone. Since the HALOE CH_4 and O_3 data were shown to be in good agreement with the whole air sampler data [*Park et al.*, 1996] and the ozone photometer data [*Brühl et al.*, 1996], it is reasonable to directly compare the two data sets.

However, it was recently suggested that mixing of subsided inner vortex air with midlatitude air alone can change initially non linear compact correlations between long-lived

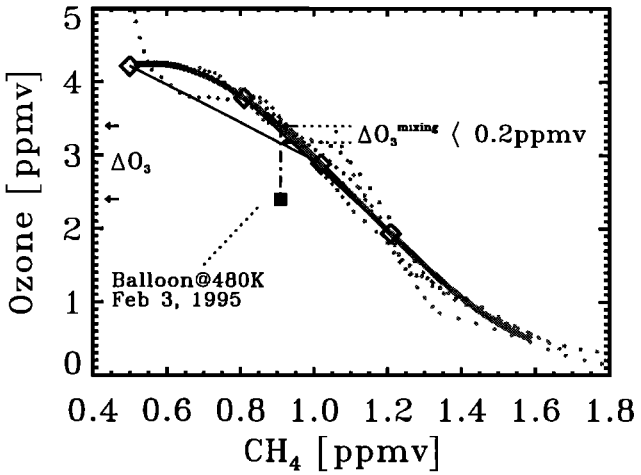

Figure 2. HALOE measurements of the CH_4-O_3 relationship in early winter 1994 (grey dots). The thick grey line gives the early winter relationship used to calculate the reference ozone mixing ratio. Also shown is the CH_4-O_3 relation observed on February 3, 1995 (solid square). Hypothetical mixing end-members, which are compatible with the N_2O-CH_4 relation observed on February 3, 1995 (see Figure 3 and text), are marked by diamonds and connected by mixing lines, which indicate how mixing alone could change the CH_4-O_3 relationship.

tracers and that the straightforward use of tracer correlations for diagnosing chemical change may substantially overestimate chemical ozone loss or denitrification, if such mixing actually takes place across the polar vortex edge [*Michelsen et al.*, 1998]. Therefore we address the question of how the air masses sampled inside the polar vortex during the balloon flight on February 3, 1995, were affected by mixing with midlatitude air and derive an upper limit of the impact of mixing on the ozone tracer correlation.

Figure 3 shows typical correlations between CH_4 and N_2O mixing ratios derived by *Michelsen et al.* [1998] using Atmospheric Trace Molecule Spectroscopy Experiment (ATMOS) satellite observations. The thick solid grey line represents the conditions as observed in the proto vortex (November 1994) and the midlatitude extra-tropic region (April 1993). The thick dash-dotted grey line represents conditions in a late vortex (April 1993) that according to *Michelsen et al.* [1998] are caused by mixing of subsided inner vortex air with midlatitude air. The CH_4/N_2O relation measured on the balloon flight of February 3, 1995, are shown as solid squares. No significant deviations of this relation from the unmixed midlatitude and proto vortex reference are found, supporting the assumption that the air masses observed during the balloon flight were not significantly influenced by mixing. To derive an upper limit of the impact of mixing on the reference correlation we have investigated the effect of different mixing scenarios that comply with the observed CH_4/N_2O relation. Two of these scenarios are illustrated in Figure 3: two air masses (diamonds) are assumed to mix, the resulting mixing ratios are indicated by the mixing lines (thin solid lines). The effect of these mixing scenarios on the CH_4-O_3 correlation is illustrated in Figure 2, with the properties of the mixing end-members of these scenarios marked as diamonds. Mixing between these possible end-members can reduce the ozone mixing ratio for the relevant CH_4 level of 0.91 ppmv at most by 0.2 ppmv as indicated by the connecting mixing lines. This value represents the upper limit of the ozone deficit that can be explained by mixing alone.

3.2. Comparison With Other Estimates of Chemical Ozone Loss

A limited number of HALOE observations of O_3 and CH_4 were made inside the Arctic polar vortex on January 26 to 28 and on February 6 and 7, 1995. We assume that the tracer compositions of air masses observed by HALOE are similar to those sampled by the in situ instruments since the PV values of the air masses were similar for both types of observations (see Table 1). These observations provide CH_4 and O_3 data, which can be combined with the early winter CH_4-O_3 correlation to quantify the ozone loss for the 480-500 K altitude range (Table 2). An average cumulative ozone loss of $\Delta O_3^{HALOE} = 0.8 \pm 0.4$ ppmv from November 1994 until early February 1995 is derived in agreement with our analysis of balloon borne observations.

Both ozone loss determinations given above are based on the assumptions that the early winter CH_4-O_3 correlation used is (1) representative of the whole polar vortex and (2) in the absence of chemical ozone loss unchanged throughout the winter. Therefore we will discuss two other, independent ozone loss determinations, which are not based

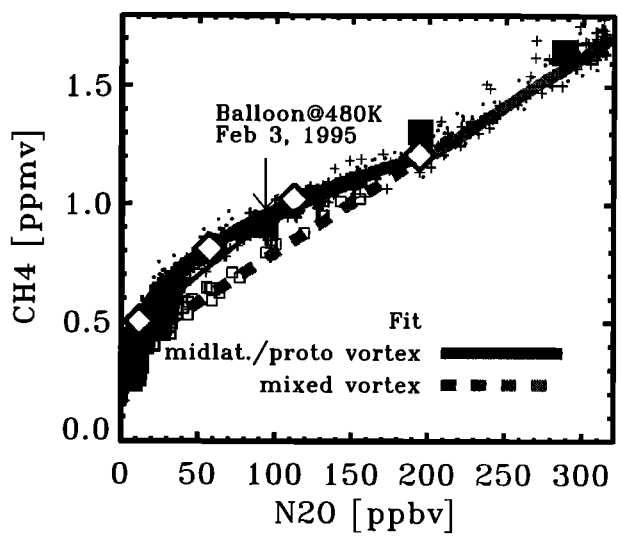

Figure 3. Shown are typical relationships between N_2O and CH_4 mixing ratios: dots, ATMOS-AT3 November 1994 midlatitude measurements; crosses, ATMOS-AT3 November 1994 proto vortex measurements; thick solid grey line, fit to the data. ATMOS-AT2 April 1993 measurements inside the vortex are shown as small grey squares, with the thick dotted grey line representing the fit to the data. ATMOS data and fits are from *Michelsen et al.* [1998]. Big solid squares indicate data of the balloon flight; large open diamonds mark hypothetical mixing end-members (see text).

Table 1. PV Values of Air Masses Sampled by Various Measurements

	Potential Vorticity, PVU					
Θ, K	Jan. 26, 1995 HALOE 49°N/38°E	Jan. 27, 1995 HALOE 50°N/132°E	Jan. 28, 1995 HALOE 51°N/132°E	Feb. 3, 1995 In Situ 64°N/25°E	Feb. 6, 1995 HALOE 47°N/58°E	Feb. 7, 1995 HALOE 45°N/58°E
400	14	19	20	12	12	13
435	21	31	31	22	22	22
475	39	47	46	44	37	38
500	53	59	56	59	51	50
550	92	80	77	90	87	79
575	113	91	88	108	112	99
600	134	102	97	135	139	119
635	163	117	108	173	184	147
675	204	132	119	216	243	188

on the tracer correlation approach. The first independent method to derive a cumulative ozone loss is the integration of ozone loss rates determined by the Match method. Integrating from January 1, 1995, a cumulative ozone loss of $\Delta O_3^{Match} = 1.1 \pm 0.2$ ppmv is derived for air masses that reside on February 3, 1995, in the altitude range from 480 to 500 K potential temperature in good agreement with the cumulative ozone loss derived from the balloon observations.

The second independent method employs ozone profile measurements made inside the Arctic polar vortex with a LIDAR at Eureka, Canada (80°N) [*Donovan et al.*, 1995] in combination with calculations of diabatic descent of air masses inside the Arctic polar vortex. We use the average ozone profile for the January 1 to January 8, 1995, period as the early winter reference and compare it to the average profile from February 14 to February 28, 1995. Air masses, which originated in January 1995 from 550 K with 3.15±0.25 ppmv ozone, would have descended to 480 K in February 1995 due to diabatic cooling [*Rex et al.*, 1999], where only 2.3±0.15 ppmv were observed. From this we deduce an ozone loss of $\Delta O_3^{Eureka} = 0.85 \pm 0.3$ ppmv. Since the average January 1995 profile reveals a nearly constant O_3 mixing ratio between 500 and 600 K potential temperature, the derived ozone loss is not very sensitive to the exact amount of diabatic descent assumed. Obviously, this will probably constitute an overestimate for early February 1995, since between February 3, 1995, and February 14-28, 1995, additional ozone loss is likely to have occurred. Determinations of ozone loss rates by the Match method [*Rex et al.*, 1999] indicate ozone loss rates ranging from about 18±6 ppbv/d around mid February 1995 and decreasing to about 8±6 ppbv/d for end of February 1995. Therefore we use an ozone loss rate of 10 ppbv/d to estimate additional ozone loss between early and late February to be 0.15 ppmv. Even with this correction the ozone loss derived from LIDAR observations is still comparable to the ozone loss derived from the balloon observations.

Table 2. Ozone Loss Between 480 and 500 K Derived From HALOE Observations

Date	CH_4, ppmv	$\hat{O}_3$, ppmv	O_3, ppmv	ΔO_3, ppmv
Jan. 26, 1995	0.86	3.6	2.6	1.0
Jan. 27, 1995	0.93	3.3	2.8	0.5
Jan. 28, 1995	0.92	3.4	2.5	0.9
Feb. 6, 1995	0.95	3.2	2.9	0.3
Feb. 7, 1995	0.87	3.6	2.9	1.3
Average				0.8±0.4

Moreover, further relevant published estimates of chemical ozone loss do also support our analysis. Using passive O_3 advected by a 3-D model, *Deniel et al.* [1998] derive a chemical ozone loss of 0.85 to 1.0 ppmv at 475 K until February 3, 1995, from a large number of satellite ozone profile observations of the Polar Ozone and Aerosol Measurement Instrument (POAM). In a similar way, *Goutail et al.* [1999] derive an chemical ozone loss of about 26% until January 30, 1995, at 475 K from balloon-borne SAOZ (Système d'Analyse pour l'Observation au Zenith) ozone profile observations, which should be compared to our 30% estimate.

All the methods discussed here probe the vortex at different locations (Eureka/HALOE/Balloon) or consider ozone loss that accumulates over a long period of time more in the sense of a vortex average (Match/POAM). However, if the ozone distribution in the Arctic polar vortex during the time period considered is quite homogeneous, as it is indicated by the Microwave Limb Sounder (MLS) ozone data [*Manney et al.*, 1996], and if all methods to estimate chemical ozone loss are reliable, it seems likely that this should cause no substantial variation of the average ozone loss derived by the different methods and the different estimates should agree. Thus it is useful to compare our ozone loss estimate with all the other available estimates of chemical ozone loss derived for the 1994/1995 winter as an additional cross check of the reliability of our analysis. We find that three independent methods of deriving a cumulative ozone loss for the early winter period based on three independent data sets and recent estimates in the literature are in agreement with our estimate derived from the in situ observations.

We note that there also exists one lower estimate of chemical ozone loss, which was derived for somewhat lower altitudes: combining MLS observations with a reverse trajectory procedure. Manney et al. [1996] calculate a chemical ozone loss of 0.5 ppmv until February 3, 1995, at 465 K. This estimate can not be directly compared with our analysis. We emphasize that the cumulative ozone loss for the appropriate lower altitudes derived from the integration of ozone loss rates as determined by the Match method is 0.55±0.15 ppmv and that almost a factor of 2 increase of ozone loss rates from altitudes of 440 to 500 K was found for the 1994/1995 winter [*Rex et al.*, 1999]. Therefore our estimate of chemical ozone loss should be a reasonable baseline to compare simulation results to.

4. Model Calculations of Ozone Loss

The simultaneous observation of the radicals ClO and BrO in combination with the quantification of the chemical ozone loss for the same air mass, which can be confirmed by other independent methods, provides a good opportunity to quantitatively test the current understanding of ozone loss processes in the polar region. Therefore we performed trajectory box model simulations using ensembles of isentropic 50 days backward trajectories on several potential temperature levels to address the following questions: Is the observed ClO profile quantitatively consistent with conversion of chlorine reservoir species to reactive chlorine on polar stratospheric clouds during the winter ? Does the model simulation reproduce the ozone loss derived from the observations ?

4.1. Model Description

The model used is a chemical box model [*Müller et al.*, 1994] with a numerical package (FACSIMILE) for stiff differential equations. It includes a complete set of gas phase and heterogeneous reactions of relevance to the stratosphere. Photolysis rates are calculated using an updated version of the scheme of *Lary and Pyle* [1991], which employs spherical geometry and multiple scattering. Heterogeneous chemistry on liquid $HNO_3/H_2SO_4/H_2O$ droplets (STS) and nitric acid trihydrate (NAT) is taken into account [*Carslaw et al.*, 1997]. For the simulations we assumed STS-PSCs unless otherwise stated. We used recommended rate constants [*DeMore et al.*, 1994] for the chemical reactions and absorption cross sections of the various species unless stated otherwise. The absorption cross sections of Cl_2O_2 are taken from *Huder and DeMore* [1995], those of HOBr from *Orlando and Burkholder* [1995], BrCl absorption cross sections from *Maric et al.* [1994], and $BrONO_2$ absorption cross sections from *Burkholder et al.* [1995].

4.2. Method

To provide meteorological input parameters for the box model, we use the U.K. Meteorological Office (UKMO) meteorological analyses and calculate ensembles of 50 day isentropic backward trajectories. We chose 10 isentropic levels (400, 435, 475, 480, 500, 550, 575, 600, 635, 675 K) and calculated ensembles of thirteen 50 days backward trajectories for each level originating on February 3, 1995, 0900 UT, within a region of 6° × 6° centered around the location of the balloon descent (64°N, 26°E).

Seasonal isentropic trajectories have been used before to calculate chemical ozone loss [*Austin et al.*, 1989]. But this approach needs some additional justification, since the trajectory calculations neglect diabatic descent known to occur inside the polar vortex [e.g., *Bauer et al.*, 1994]. In addition, trajectories in the middle stratosphere can be considered quantitatively accurate for only up to about 10 days [*Austin*, 1986]. The error of the calculated air parcel position increases with time due to propagation of errors [*Knudsen and Carver*, 1994]. Therefore the photochemical and/or temperature history represented by a single 50 day trajectory might differ from that experienced over the winter by the air sampled during the balloon flight.

Nevertheless, provided the isentropic gradient in tracer mixing ratios across the vortex edge, for example enhanced Cl_y compared to out-of-vortex air masses, due to diabatic descent is taken into account for the initialization of chemical species, this approach is reasonable: 50 days isentropic backward trajectories can be considered a good first approximation of photochemical and temperature history for the following arguments. (1) Since the procedure is based on the meteorological analysis, the conditions along the trajectories approximate to the large-scale pressure and temperature fluctuations and photochemical conditions experienced by the air masses sampled during the balloon flight. (2) The polar vortex was elongated but mostly centered over the pole from mid December 1994 until mid January 1995, so that the polar vortex was mostly in darkness throughout that time period. Thus during early winter the photochemical evolution of most air parcels inside the polar vortex should not be strongly influenced by their exact location. During the second half of January 1995 the vortex was located over Siberia receiving more solar insolation than in early winter, so that the precise solar zenith angle describing the insolation of an air parcel inside the vortex becomes more important. However, air parcel positions calculated for the final 2 weeks prior to balloon flight should be quite accurate, because this time period is reasonably short. (3) Since extremely low temperatures extended over a large part of the polar vortex [*Naujokat and Pawson*, 1996] and over a wide vertical range (475 to 600 K potential temperature), air parcels circulating inside the vortex have most likely encountered the same low temperatures irrespective of their exact location. (4) Since we employ an ensemble of trajectories to simulate the processing of chlorine reservoir species and the ozone loss during the winter, we consider an ensemble of possible photochemical and temperature histories for the air masses sampled during the balloon flight. Thus the simulation results are more generally applicable to the air masses within which the balloon measurements were obtained.

4.3. Initialization

The initialization of chemical species, representative of early winter conditions, is shown in Table 3. It is mostly

Table 3. Initialization of Chemical Species as Used for the Model Study

	Θ, K									
	400	435	475	480	500	550	575	600	635	675
N_2O, ppb	244	172	104	93	78	38	17	7	7	7
CH_4, ppm	1.49	1.22	0.95	0.91	0.81	0.53	0.40	0.28	0.28	0.28
O_3, ppm	0.74	1.88	3.21	3.39	3.78	4.24	(4.30)	(4.30)	(4.30)	(4.30)
Cl_y, ppb	1.60	2.59	3.15	3.21	3.27	3.36	(3.35)	(3.34)	(3.34)	(3.34)
$ClONO_2$, ppb	1.17	1.53	1.43	1.4	1.25	0.98	(0.75)	(0.54)	(0.54)	(0.54)
HCl, ppb	0.44	1.05	1.72	1.81	2.02	2.38	(2.60)	(2.80)	(2.80)	(2.80)
HCl/Cl_y	0.27	0.41	0.55	0.56	0.62	0.71	(0.78)	(0.84)	(0.84)	(0.84)
H_2O, ppm	4.0	4.5	5.0	5.1	5.3	5.8	(6.2)	(6.5)	(6.5)	(6.5)
NO_y, ppb	4.3	8.2	13.3	13.3	16.2	(15.9)	(13.2)	(10.4)	(10.4)	(10.4)
HNO_3, ppb	2.5	5.4	9.5	9.5	11.9	(11.9)	(9.9)	(7.9)	(7.9)	(7.9)
N_2O_5, ppb	0.31	0.67	1.19	1.19	1.49	(1.49)	(1.24)	(0.99)	(0.99)	(0.99)
Br_y, ppt	10	15	20	20	20	20	20	20	20	20
ASFC, $10^{-8}cm^{-1}$	1.1	0.7	0.3	0.3	0.2	0.1	0.1	0.1	0.07	0.05

Numbers in parentheses are not derived from tracer correlations (see text).

based on observations: empirically derived correlation functions between the mixing ratios of a long-lived tracer, that is, CH_4 or N_2O, and the species of interest were combined with the in situ measurements of the tracers linearly interpolated to the appropriate potential temperature. By using this tracer correlation approach we obtained the initial chemical composition appropriate for descending air masses: We neglect diabatic descent for the trajectory calculations but do take account of it for the chemical composition of the air masses.

Cl_y was calculated from N_2O mixing ratios using the expression $Cl_y = 3322 + 2.35 \times N_2O - 0.0385 \times N_2O^2$ (Cl_y in pptv, N_2O in ppbv, valid for N_2O=20-300 ppbv), which was derived from three Arctic observations made by whole air samplers in the 1994/1995 winter. The HCl mixing ratio was calculated using the expression $HCl = 1.87 \times CH_4^3 - 6.57 \times CH_4^2 + 5.14 \times CH_4 + 1.16$ (HCl in ppbv, CH_4 in ppmv, valid for CH_4= 0.6-1.5 ppmv) derived from HALOE early winter observations made in November 1994 inside the Arctic polar vortex. The difference between Cl_y and HCl was assumed to be $ClONO_2$. This procedure gave HCl to Cl_y ratios of 33% on the 400 K level rising up to 65% on the 550 K level consistent with findings from *Dessler et al.* [1995] and *Engel et al.* [1997], which also indicate that above 20 km the dominant chlorine reservoir is HCl. Outside the validity range of the correlation above 550 K we assumed 3.4 ppbv Cl_y with an HCl/Cl_y ratio of 0.7 to 0.85 increasing with altitude (between 550 and 675 K) consistent with mid latitude observations made in November 1994 by the ATMOS instrument during the ATLAS 3 mission [*Zander et al.*, 1996].

The total bromine loading was assumed to be 11 and 15 pptv on the 400 and 435 K level and 20 pptv above, consistent with the findings of *Wamsley et al.* [1998] and is initialized as $BrONO_2$.

NO_y was taken from a correlation between N_2O and NO_y derived from midlatitude observations (44°N) in fall 1994 [*Kondo et al.*, 1996]. Above 550 K N_2O mixing ratios were again below the lower limit of validity of the correlation. ATMOS measurements were used to estimate the amount of NO_y [*Rinsland et al.*, 1996]. HNO_3 was assumed to be 80% of NO_y minus $ClONO_2$, the remainder being N_2O_5 [*Kawa et al.*, 1992].

H_2O was initialized by use of a correlation with CH_4 derived during the European Arctic Stratospheric Ozone Experiment (EASOE) in 1991/1992 by *Engel et al.* [1996]. The initial background aerosol surface area was taken to be the average of in situ observations made during the SESAME campaign [*Deshler and Oltmans*, 1998]. O_3 was initialized using the early winter 1994 correlation function derived from HALOE observations, which was also used to derive the ozone loss. Outside the validity range of the correlation we initialized with 4.3 ppmv ozone.

5. Model Results

5.1. General Remarks

Our main focus is the comparison of the simulated chemical composition of air masses with the observations made on February 3, 1995. From the ClO measurements, three altitude ranges can be distinguished: above, inside, and below the layer of enhanced ClO mixing ratios. This classification is used for the discussion of the properties of the trajectories as well. On the isentropic surfaces above the layer of enhanced ClO mixing ratios (600, 635, and 675 K) the average minimum temperatures within each trajectory ensemble are 188.1±0.8, 188.8±0.5, and 190.5±0.8 K. Despite these low temperatures, the low H_2O and HNO_3 partial pressures at these altitudes are not favorable for PSC formation. On isentropic surfaces within the layer of enhanced ClO mixing ratios (475, 500, and 550 K) the average minimum temperature within the trajectory ensembles is about 188.0±1.0 K. At these altitudes the minimum temperatures along a trajectory, which are comparable to the vortex minimum temperatures [*Naujokat and Pawson*, 1996], are typically reached in the second half of December 1994. In the simulations the repeated occurrence of these cold temperatures triggers

multiple PSCs events for the air parcels, so that a complete processing is accomplished for most of the trajectories on these levels. The minor stratospheric warming taking place at the end of January 1995 is also represented in the temperature history of the trajectory ensemble. Based on PV arguments, calculated air parcel positions are clearly inside the polar vortex. Below the layer of enhanced ClO mixing ratios (400 and 435 K) the trajectories can be separated into in-vortex, vortex-edge, and out-of-vortex trajectories, with respectively different temperature histories. Out-of-vortex temperature histories are generally too warm for PSC existence (T_{min} >200 K), while minimum temperatures for the other trajectories range from 190 to 195 K.

With regard to the amount of sunlight encountered, the trajectory ensemble is also comparable to the vortex average. We define the mean sunlit time per day (MST) of a trajectory as the fraction of time with solar zenith angles below 95° within a 24 h interval. Averaging MST over the trajectory ensemble of an isentropic surface yields values of about 0.1 in early January 1995 increasing to about 0.3 at the end of January 1995 roughly consistent with the vortex mean sunlit time per day [*Rex et al.*, 1999]. This increase in solar insolation along the trajectories is reflected in the simulated time evolution of ozone. Large ozone losses are typically simulated for the second half of January 1995, with minor losses before.

Since we use an ensemble of isentropic trajectories that provides reasonable photochemical and temperature histories, which are consistent with typical features of the polar vortex, the simulation results should be applicable to observations made during the balloon flight on February 3, 1995.

5.2. Halogen Species

Figure 4a shows the HCl simulations for February 3, 1995, 0900 UT, for all trajectories within the ensemble. Also shown is the range of observations of HCl made inside the Arctic polar vortex by HALOE on January 26 to 28 and on February 6 and 7, 1995. Given that the air parcels have similar values of PV (see Table 1), we again assume that the tracer composition of air masses observed by HALOE is comparable to those sampled by the in situ instruments on February 3, 1995. Furthermore, due to the minor stratospheric warming the temperatures during that period were too high to allow for further PSC processing and the time between the HALOE and the in situ measurements was too short for significant chemical recovery of HCl. Thus the HALOE and in situ measurements may be combined. The general shape of the observed HCl profile is well simulated by the model. At the lower altitudes, where mixing processes might have interfered, and on the upper four model levels, where the initialization of chlorine species is less certain, simulated and observed HCl are not in particularly good agreement. At altitudes between 475 and 550 K, that is, where the ozone loss was observed, the simulated and measured HCl are in good agreement giving confidence in the model representation of the heterogeneous conversion

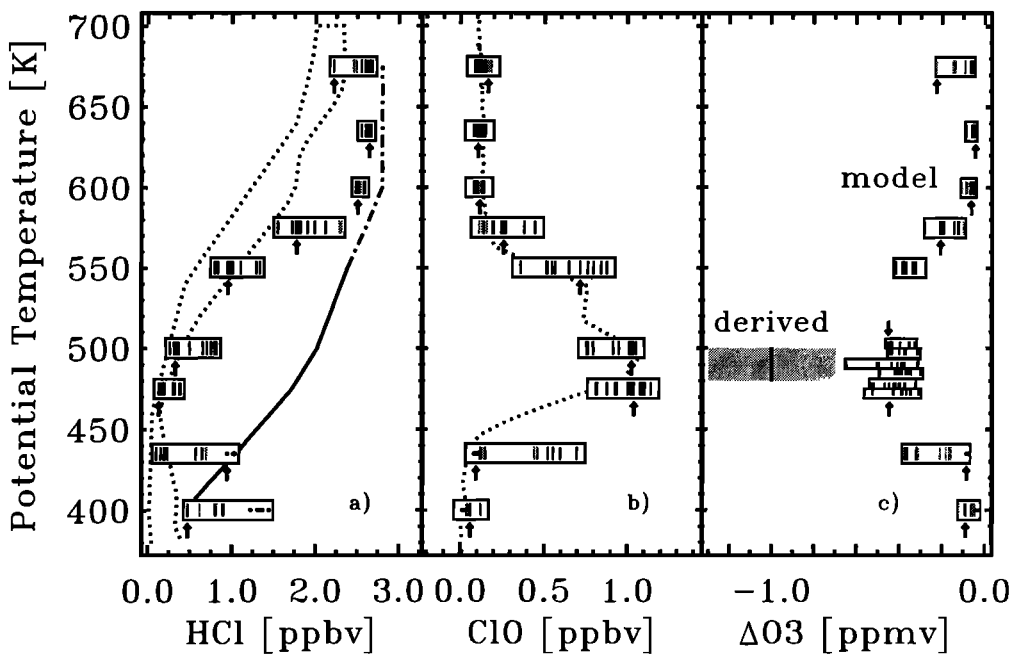

Figure 4. (a) Simulated HCl mixing ratios. The area enclosed by the dotted lines shows the range of HCl mixing ratios as observed by HALOE in January/February 1995, and the solid line shows the initialization used for the model runs. (b) Simulated ClO mixing ratios compared to the observed ClO mixing ratio (black dotted line). (c) simulated cumulative ozone loss compared to the derived ozone loss. The horizontal boxes indicate the range of simulation results. Individual results of the trajectories are marked; the position of the trajectories relative to the vortex edge is coded: out of vortex, solid dot; vortex edge, dark grey vertical line; inside vortex, solid vertical line. The arrows mark results of the trajectories ending at the location of the descent measurement.

of chlorine reservoir species to reactive chlorine on polar stratospheric clouds, especially for that altitude.

Figure 4b shows simulated ClO mixing ratios valid for 0900 UT and the ClO profile as measured on the parachute descent, which took place between 0845 and 0915 UT. A quantitative agreement between simulated and measured ClO is achieved, which is particularly good at the levels where the ozone loss was observed. At 550 K the simulations cover the range of ClO mixing ratios observed within the region of the steep ClO gradient. Higher up on the 575 K level the simulations indicate ClO mixing ratios ranging from 110 to 445 pptv compared to observed 150 pptv. However, this overestimate on some of the trajectories is within the uncertainties implied by the input parameters as shown in the sensitivity study described below.

Measured BrO mixing ratios were 9-10 pptv between 475 and 675 K. The simulations slightly overestimate BrO with simulated mixing ratios of 10-13 pptv for these altitudes, but are still within the ±30 % error of the BrO observations.

5.3. Simulated Ozone Loss

For the simulated O_3 loss, in addition to the trajectories around the location of the descent observations, trajectories on the 475, 480, and the 500 K level were calculated originating around the location of ascent (68°N, 21°E), and corresponding simulation runs were made. The combined results of simulated O_3 loss are plotted in Figure 4c. The average simulated O_3 loss on isentropic levels in the 475 to 500 K potential temperature range is 0.4±0.1 ppmv (1σ standard deviation). The contributions of the ClO dimer and the BrO-ClO cycle are about 40% and 38% , respectively, in agreement with other simulation results [*Chipperfield and Pyle*, 1998]. The ozone loss derived from observations for the 480 K level was 1.0±0.3 ppmv (section 3). The simulations underestimate the observed ozone loss by approximately a factor of 2.

5.4. Sensitivity Studies

Although the initialization values of most chemical species are constrained by observations, some uncertainties remain. The key uncertainties are the initial aerosol surface area density (ASFC), which controls the reaction rates of heterogeneous reactions under background conditions, and the amount of HNO_3 together with the synoptic temperature as these parameters mainly control the PSC processing. In order to evaluate the possible influence of these uncertainties on the model results, we performed a sensitivity study varying these parameters within reasonable limits. As the model results of the different trajectories within each ensemble were very similar, only the set of trajectories ending at the location of the descent measurement was used for the sensitivity study. The results of the sensitivity study are shown in Figure 5.

Simulations using either half or double the initial surface area density (ASFC) as in the base run (Table 1) were performed. The simulations indicate that results for isentropic

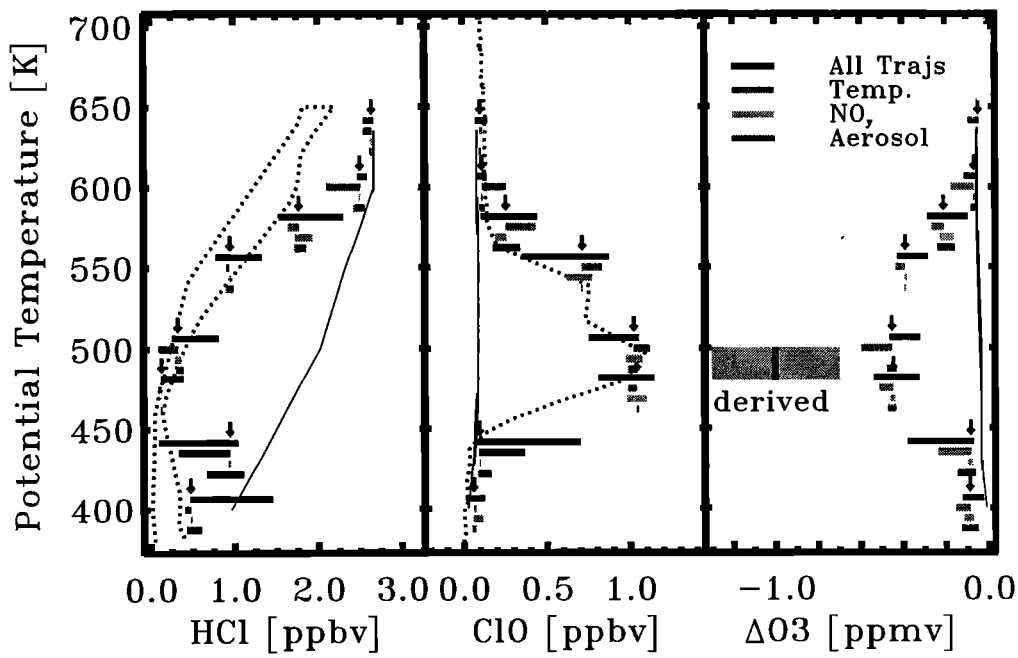

Figure 5. Results of the sensitivity study: Shown is the range of the simulated HCl and ClO mixing ratios and the simulated ozone loss induced by the variation of input parameters (temperature, -1 K, -2 K; NO_y, ±2 ppbv; aerosol, ×2, $\times\frac{1}{2}$) compared to the range of results for model runs using the set of trajectories ending around the location of the descent measurement (dotted line). The arrows mark the results of the one trajectory set used for the sensitivity study with input parameters unchanged. The runs were performed assuming a liquid PSC scheme. Results of a pure gas phase chemistry run are shown by the thin solid line.

levels inside the layer of enhanced ClO mixing ratios (475, 500, and 550 K), where the local ozone minimum was observed, are insensitive to the initial aerosol surface density. In contrast, results for isentropic levels below the layer of enhanced ClO mixing ratios are sensitive to this parameter. On the two lowest levels (400 and 435 K) the temperatures are so high that only a slight increase in aerosol surface density is simulated during cold periods, so that most of the processing takes place on background surface aerosol and the initial aerosol loading translates directly into the amount of HCl lost. Between 475 and 550 K the minimum temperatures are so low that PSCs form. The available surface area density increases by 1 order of magnitude during PSC periods with the maximum values reached being nearly independent of the initial aerosol surface area and processing continues until one of the reactants is used up. On the 575 and 600 K level the situation is different, because the aerosol surface area density is somewhat enhanced, when the minimum temperatures on the trajectory are reached. But the maximum size and therefore the amount of processing during PSC events still depends on the initial surface area density. At these levels, reducing the aerosol surface density by a factor of 2, leads to a decrease of the simulated ClO mixing ratio on the 575 K level from 260 pptv to 180 pptv, which is somewhat closer to the measured value of 150 pptv. On the 635 and 675 K level the surface area densities are so small that no significant heterogeneous chemistry occurs; consequently, these simulations are virtually indistinguishable from those simulating only pure gas phase chemistry.

As the exact microphysical nature of PSCs is still not well known, in addition to the standard simulations assuming liquid PSCs simulations assuming a NAT formation at 3 K supercooling below the NAT equilibrium point [*Hanson and Mauersberger*, 1988] were performed. The results (not shown) are very similar to the liquid aerosol case, so that the subsequent discussion of model results is limited to the liquid PSC case but is relevant for both PSC schemes.

Another important parameter is the HNO_3 mixing ratio, since the PSC existence and surface area density depend on the HNO_3 partial pressure. Using the correlation approach, only NO_y can be derived and the amount of HNO_3 within the NO_y family has to be estimated. We have performed sensitivity studies, where we have varied the amount of NO_y by ± 2.0 ppbv keeping the assumed initial partitioning. As HNO_3 is the major species within the NO_y family, this variation is equivalent to a variation of the HNO_3 amount itself. The sensitivity due to the variation in HNO_3 is again within the limits of the variability given by the use of different trajectories (Figure 5).

As denitrification processes were shown to have occurred in the 1994/1995 winter [*Sugita et al.*, 1998], additional runs were performed accounting for this effect, by simulating HNO_3 removal in the model during PSC existence periods. Although this leads to an increase of simulated ClO mixing ratios of about 200 pptv on February 3, 1995, the effect on the cumulative ozone loss over the 50 day model period is less than 0.1 ppmv.

Heterogeneous processing does critically depend on temperatures. A sensitivity study on temperatures is implied by the use of an ensemble of trajectories with a variability in temperature. However, there are suggestions of a positive bias of the UKMO analysis temperatures relative to radiosonde temperatures with UKMO temperatures being about 2 K too high [*Pullen and Jones*, 1997]. Therefore simulations were performed with the UKMO synoptic temperatures reduced by 1 and 2 K. This variation only affects results on the 435, 575, and 600 K level, where temperatures along the trajectories are close to the PSC formation temperature. Reducing the temperature leads to an an increase in simulated ClO mixing ratios from about 100 pptv to at most 400 pptv. On model levels, where the discrepancy between simulated and derived ozone loss is observed, the temperatures given by the trajectories are well below the PSC formation temperature, so that the total chlorine processing and the simulated ozone loss are insensitive to these temperature variations.

These tests show that the variability in the model results of a single set of trajectories, which is introduced by the uncertainty of various input parameters (aerosol loading, HNO_3 mixing ratio, temperature), is well represented by the use of an ensemble of isentropic trajectories. Furthermore, the results of the model study are insensitive to uncertainties in the values of the input parameters.

6. Discussion

Our analysis reveals a significant discrepancy between simulated and derived cumulative ozone loss despite a good agreement between simulated and observed mixing ratios of key species in chemical ozone destruction, ClO and BrO. In principle, the disagreement could be caused by errors in determining the cumulative ozone loss or by systematic errors in the model study or by both.

We have shown (section 3) that three independent methods of deriving a cumulative ozone loss for the early winter period are in good agreement. Therefore it is unlikely that the ozone loss determination is erroneous.

We next have to check the validity of the model study, which is based on the assumption that the use of an ensemble of isentropic 50 days backward trajectories calculated from the meteorological analysis provides a suitable history of the air masses observed during the balloon flight inside the Arctic polar vortex. This assumption is a posteriori justified by showing that typical characteristics of the temperature and photochemical history represented by the trajectory ensembles are comparable to vortex averages. However, since ozone loss is proportional to the time spent in sunlight [*Rex et al.*, 1999] and since the true histories of the observed air masses need not necessarily be the vortex average, a possible explanation of the discrepancy between derived and simulated cumulative ozone loss could be that the trajectories used underestimate the total amount of sunlight.

But we can show that the observed discrepancy between derived and simulated ozone loss is not likely only due to an

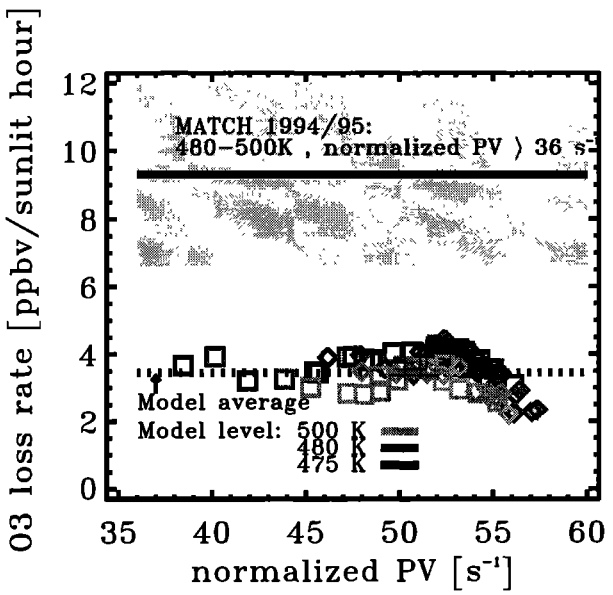

Figure 6. Simulated ozone loss rates along the trajectories averaged over days 23-33 of 1995 versus normalized PV. The potential temperature level of the trajectories is color coded; squares, trajectories ending around the location of descent; diamonds, trajectories ending around the location of ascent; dotted line, model average. Also shown is the result of the Match analysis valid for the same time and the altitude range of 480-500 K (solid line).

erroneous representation of photochemical and/or temperature history inside the Arctic polar vortex by our trajectory ensemble. Since trajectory calculations may be considered reasonable for up to 10 days [*Austin*, 1986], ozone loss rates derived from the simulations for the final 10 days prior to the measurement should not be severely biased by trajectory errors and can be compared with ozone loss rates derived from the Match analysis, which have been interpreted as a vortex average. Match ozone loss rates are determined by performing a linear least squares fit to observed ozone mixing ratios as a function of time spent in sunlight using a large number of pairs of ozone observations linked by trajectory calculations [*Rex et al.*, 1999]. We therefore determine the ozone loss rates in the model by performing a linear least squares fit of simulated ozone mixing ratios versus time spent in sunlight along a trajectory using the data of the last 10 days prior to the measurement (days 23-33 of 1995). Results of this analysis for the trajectories on 475, 480, and 500 K are shown in Figure 6 as a function of normalized PV as defined by *Rex et al.* [1999], compared to the Match analysis for the 480-500 K altitude range, which is valid for days 23-33 of 1995. Simulated and derived ozone loss rates differ by approximately a factor of 2 consistent with the factor of 2 discrepancy in the cumulative ozone loss observed before, but with the advantage that the meteorological conditions for the determination of the simulated loss rates are less uncertain than those used for the determination of the simulated cumulative ozone loss. This finding is also in agreement with the study by *Becker et al.* [1998], in which a much more thorough comparison of ozone loss rates derived from the Match analysis with simulated ozone loss rates for the 1991/1992 winter is presented and likewise a large discrepancy between simulated and derived ozone losses was found for the early winter period.

Finally, we have calculated ozone loss rates for idealized conditions particularly favorable for ozone loss. We assume air parcels containing initially 3 ppbv ClO that for 10 days (days 23-33, 1995) are at constant latitudes (50, 55, 60, and 65°N) with constant pressure (50 hPa) and temperatures (195, 205, and 215 K) corresponding to potential temperatures of 460, 485, and 505 K. To check the influence of a possible denitrification, which would slow the recovery of chlorine reservoir species, we assume different HNO_3 mixing ratios of 2, 7, and 14 ppbv. Moreover, model calculations were performed using Cl_2O_2 absorption cross sections as measured by *Huder and DeMore* [1995] and as recommended by *DeMore at al.* [1994]. The results are shown in Figure 7. We find that only in the cases of extremely low HNO_3 mixing ratios of 2 ppbv, which are typical for the Antarctic polar vortex [*Fahey et al.*, 1990], the simulated ozone loss rates are comparable to the lower limit of the Match analysis. But observations in the 1994/1995 winter reveal on average 4-5 ppbv NO_y for the theta levels of interest, when denitrification occurs [*Sugita et al.*, 1998]. With

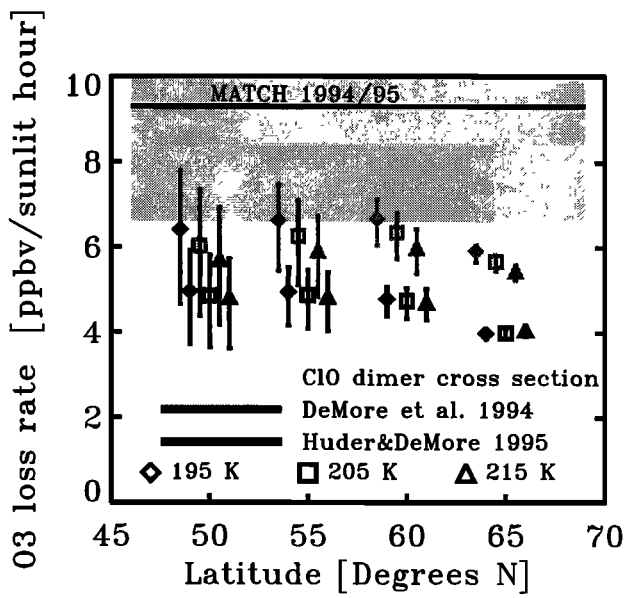

Figure 7. Simulated ozone loss rates under idealized conditions (see text) averaged over days 23-33 of 1995 assuming an air parcel at fixed latitude with constant pressure of 50 hPa and constant temperature of 195, 205, or 215 K. The symbols show results assuming 7 ppbv HNO_3; the error bars show the range of ozone loss rates derived with different assumptions on HNO_3 mixing ratio: 2 ppbv (upper limit) and 14 ppbv (lower limit). Results of calculations using *Huder and DeMore* [1995] ClO dimer absorption cross sections are shown in black, and those using *DeMore et al.* [1994] recommendations in grey. Also shown is the result of the Match analysis valid for the same time and the altitude range of 480-500 K.

7 ppbv HNO_3 at most the lower limit of the ozone loss rates derived from Match can be achieved in the model, and this only in the very unrealistic case of a constant temperature of 195 K. With 14 ppbv HNO_3 the loss rates derived from the Match analysis are not reproduced in any of the assumed cases.

We find that even under idealized conditions favorable for ozone loss, the model severely underestimates the ozone loss rates compared to observations. Thus we conclude that the difference between simulated and derived cumulative ozone loss can not be explained solely by an underestimate of the amount of sunlight represented by the trajectories.

7. Summary and Conclusions

An analysis of simultaneous profile observations of ClO, BrO, O_3, and long-lived tracers in the Arctic vortex, performed with a combined balloon payload launched from Kiruna, Sweden, on February 3, 1995, is presented. Using as a reference a correlation function between CH_4 and O_3 mixing ratios derived from HALOE observations in the Arctic polar vortex in November 1994, a chemical ozone loss of 1.0± 0.3 ppmv was derived for the 480 K level (21 km). This ozone loss coincides with a layer of enhanced ClO mixing ratios.

In order to check the quantitative understanding of ozone loss processes, model simulations of the time evolution of the chemical composition of the lower stratosphere were conducted. We conclude that the observed ClO profile is consistent with heterogeneous conversion of reservoir chlorine species on polar stratospheric clouds. In addition, the simulated HCl mixing ratios were shown to be in good agreement with observations of HCl in the Arctic polar vortex, indicating that the partitioning of the inorganic chlorine family is well simulated by the model. The model was also shown to reproduce the observed BrO profile. However, the model simulations indicate a cumulative ozone loss of 0.4±0.1 ppmv in the altitude region of the enhanced ClO mixing ratios (21 km, equivalent to 480 K), which is only approximately half the cumulative ozone loss derived from observations.

We have shown that the cumulative ozone loss of 1.0±0.3 ppmv derived from the singular profile observations made during the balloon flight on February 3, 1995, is consistent with published estimates and with estimates based on other data sets. Analyzing independent satellite profile observations using the same early winter CH_4-O_3 correlation as a reference gives a cumulative ozone loss of 0.8±0.4 ppmv. Additional estimates of cumulative ozone loss, that confirm our estimate, but are not based on the tracer correlation technique, were also presented: $0.85^{+0.3}_{-0.45}$ ppmv deduced from profile observations of ozone at Eureka, Canada, 80°N, taking diabatic descent into account and 1.1±0.2 ppmv from the integration of ozone loss rates derived from the Match analysis.

As the simulated ozone loss depends critically on the specific details of the photochemical and temperature history of air masses, which, although unlikely, might not be appropriately represented by the 50 days isentropic backward trajectories used, we have further compared simulated ozone loss rates, which are averaged for the last 10 days before our measurement, with ozone loss rates derived from the Match observations for the same period of time. Again we find approximately a factor of 2 difference between simulated and derived ozone loss rates. In addition, we have shown that even under idealized conditions, highly favorable for ozone loss, simulations can not reproduce the ozone loss rates derived from the Match analysis. Discrepancies between simulated and derived ozone loss were observed before in 3-D model studies [*Hansen et al.*, 1997; *Goutail et al.*, 1999; *Deniel et al.*, 1998], and it was suggested that this might be a resolution problem in the 3-D model [*Edouard et al.*, 1996]. We emphasize that a box model does not have this resolution problem.

These findings indicate that there are either fundamental but not yet identified flaws in all the techniques used to derive ozone loss that have been employed in this paper, or that at least for the early winter period and the altitude region (21 km, equivalent to 480 K) discussed the currently accepted paradigm of ozone loss in the polar regions as a result of the catalytic action of halogen radicals due to the ClO dimer and the BrO-ClO cycle is not a complete description of the ozone loss processes relevant to the winter polar vortex.

Acknowledgments. The authors thank D. W. Toohey, J. M. Pierson, and K. A. McKinney for their hard work to produce a first class ClO/BrO data set, the HALOE team for providing HALOE data, H. A. Michelsen for providing the ATMOS data, and D. Donovan for the LIDAR ozone data. Superb operational work during the balloon campaign by the CNES and ESRANGE teams is gratefully acknowledged. Part of the work was funded by the BMBF.

References

Anderson, J.G., D.W. Toohey, and W.H. Brune, Free radicals within the Antarctic vortex: the role of CFCs in the Antarctic ozone loss, *Science, 251,* 39-46, 1991.

Austin, J., Comparison of stratospheric air parcel trajectories calculated from SSU and LIMS satellite data, *J. Geophys. Res., 91,* 7837–7851, 1986.

Austin, J., et al., Lagrangian photochemical modeling studies of the 1987 Antarctic spring vortex, 2, Seasonal trends in ozone, *J. Geophys. Res., 94,* 16717–16735, 1989.

Bauer, R., A. Engel, H. Franken, E. Klein, G. Kulessa, C. Schiller, U. Schmidt, R. Borchers, and J. Lee, Monitoring the structure of the Arctic polar vortex over northern Scandinavia during EASOE: Regular N_2O profile observations, *Geophys. Res. Lett., 21,* 1211-1214, 1994.

Becker, G., R. Müller, D. McKenna, M. Rex, and K. Carslaw, Ozone loss rates in the Arctic stratosphere in the winter 1991/92: Model calculations compared with Match results, *Geophys. Res. Lett., 25,* 4325-4328, 1998.

Burkholder, J.B., A.R. Ravishankara, and S. Solomon, UV/visible and IR absorption cross sections of $BrONO_2$, *J. Geophys. Res., 100,* 16793-16800, 1995.

Brühl, Ch., et al., Halogen occultation experiment ozone channel validation, *J. Geophys. Res., 101,* 10217-10240, 1996.

Brune, W.H., J.G. Anderson, and K.R. Chan, In situ observations of BrO over Antarctica: ER-2 aircraft results from 54°S to 72°S latitude, *J. Geophys. Res., 94,* 16639–16647, 1989.

Brune, W.H., D.W. Toohey, J.G. Anderson, J.G., and K.R. Chan, In situ observations of ClO in the Arctic stratosphere: ER-2 aircraft results from 59°N to 80°N latitude, *Geophys. Res. Lett., 17,* 505-508, 1990.

Brune, W.H., J.G. Anderson, D.W. Toohey, D.W. Fahey, S.R. Kawa, R.L. Jones, D.S. McKenna, and L.R. Poole, The potential for ozone depletion in the Arctic stratosphere, *Science, 252,* 1260-1266, 1991.

Carslaw, K.S., T. Peter, and R. Müller, Uncertainties in reactive uptake coefficients for solid stratospheric particles, 2, Effect on ozone depletion, *Geophys. Res. Lett., 24,* 1747-1750, 1997.

Chipperfield, M.P., and J.A. Pyle, Model sensitivity studies of Arctic ozone depletion, *J. Geophys. Res., 103,* 28389-28403, 1998.

DeMore, W.B., S.P. Sander, D.M. Golden, R.F. Hampson, M.J. Kurylo, C.J. Howard, A.R. Ravishankara, C.E. Kolb, and M.J. Molina, Chemical kinetics and photochemical data for use in stratospheric modelling, *Eval. 11, JPL Publ., 94-26,* 1994.

Deniel, C., R.M. Bevilacqua, J.P. Pommereau, and F. Lefèvre, Arctic chemical ozone depletion during the 1994-95 winter deduced from POAM II satellite observations and the REPROBUS three-dimensional model, *J. Geophys. Res., 103,* 19231-19244, 1998.

Deshler, T., and S.J. Oltmans, Vertical profiles of volcanic aerosol and polar stratospheric clouds above Kiruna, Sweden: Winters 1993 and 1995, *J. Atmos. Chem., 30,* 11-23, 1998.

Dessler, A.E., et al., Correlated observations of HCl and $ClONO_2$ from UARS and implications for stratospheric chlorine partitioning, *Geophys. Res. Lett., 22,* 1721-1724, 1995.

Donovan, D.P., J.C. Bird, J.A. Whiteway, T.J. Duck, S.R. Pal, and A.I. Carswell, Lidar observations of stratospheric ozone and aerosol above the Canadian high Arctic during the 1994-1995 winter, *Geophys. Res. Lett., 22,* 3489-3492, 1995.

Edouard, S., B. Legras, F. Lefèvre, and R. Eymard, The effect of small-scale inhomogeneities on the ozone depletion in the Arctic, *Nature, 384,* 444-447, 1996.

Engel, A., C. Schiller, U. Schmidt, R. Borchers, H. Ovarlez, and J. Ovarlez, The total hydrogen budget in the Arctic winter stratosphere during the European Arctic Stratospheric Ozone Experiment, *J. Geophys. Res., 101,* 14495-14503, 1996.

Engel, A., U. Schmidt, and R. Stachnik, Partitioning between chlorine reservoir species deduced from observations in the Arctic winter stratosphere, *J. Atmos. Chem., 27,* 107-126, 1997.

Fahey, D.W., S. Solomon, S.R. Kawa, M. Loewenstein, J.R. Podolske, S.E. Strahan, and, K.R. Chan A diagnostic for denitrification and dehydration in the polar winter stratosphere, *Nature, 345,* 698-702, 1990.

Farman, J.C., B.G. Gardiner, and J.D. Shanklin, Large losses of total ozone in Antarctica reveal seasonal ClO_x/NO_x interaction, *Nature, 315,* 207-210, 1985.

Goutail, F., et al., Depletion of column ozone in the Arctic during the winters of 1993-94 and 1994-95, *J. Atm. Chem., 32,* 1-34, 1999.

Hansen, G., T. Svenøe, M. Chipperfield, A. Dahlback, U.-P. Hoppe, Evidence of substantial ozone depletion in winter 1995/96 over Northern Norway, *Geophys. Res. Lett., 24,* 799-802, 1997.

Hanson, D.R., and K. Mauersberger, Laboratory studies of the nitric acid trihydrate: Implications for the south polar stratosphere, *Geophys. Res. Lett., 15,* 855-888, 1988.

Huder, K., and W.B. DeMore, Absorption cross sections of the ClO dimer, *J. Phys. Chem., 99,* 3905-3908, 1995.

Kawa, S.R., et al., Photochemical partioning of the reactive nitrogen and chlorine reservoirs in the high-latitude stratosphere, *J. Geophys. Res., 97,* 7905-7923, 1992.

Kelly, K.K., et al., Dehydration in the lower Antarctic stratosphere during the late winter and early spring, *J. Geophys. Res., 94,* 11317–11357, 1989.

Knudsen, B., and G. Carver, Accuracy of the isentropic trajectories calculated for the EASOE campaign, *Geophys. Res. Lett., 21,* 1199-1202, 1994.

Kondo, Y., U. Schmidt, T. Sugita, A. Engel, M. Koike, P. Aimedieu, M.R. Gunson, and J. Rodriguez, NO_y correlation with N_2O and CH_4 in the midlatitude stratosphere, *Geophys. Res. Lett., 23,* 2369-2372, 1996.

Lary, D.J., and J.A. Pyle, Diffuse radiation, twilight and photochemistry, *J. Atmos. Chem., 13,* 373-406, 1991.

Lefévre, F., F. Figarol, K. Carslaw, and T. Peter, The 1997 Arctic ozone depletion quantified from three dimensional model simulations, *Geophys. Res. Lett., 25,* 2425-2428, 1998.

Manney, G.L., et al., Arctic ozone depletion observed by UARS MLS during the 1994-1995 winter, *Geophys. Res. Lett., 23,* 85-88, 1996.

Maric, D., J.P. Burrows, and G.K. Moortgat, A study of the UV-visible absorption spectra of Br_2 and BrCl, *J. Photochem. Photobiol., 83,* 179-192, 1994.

McElroy, M.B., R.J. Salawitch, S.C. Wofsy, and J.A. Logan, Antarctic ozone: Reductions due to synergistic interactions of chlorine and bromine, *Nature, 321,* 759-762, 1986.

McKenna, D.S., et al., Calulations of ozone destruction during the 1988/1989 arctic winter, *Geophys. Res. Lett., 17,* 553-556, 1990.

McKinney, K.A., J.M. Pierson, and D.W. Toohey, A wintertime in situ profile of BrO between 17 and 27 km in the Arctic vortex, *Geophys. Res. Lett., 24,* 853-856, 1997.

Michelsen, H.A., Manney, G.L., M.R. Gunson, and R. Zander, Correlations of stratospheric abundances of NO_y, O_3, N_2O, and CH_4 derived from ATMOS measurements, *J. Geophys. Res., 103,* 28347–28359, 1998.

Molina, M.J., T.-L. Tso, L.T. Molina, and F.C.-Y. Wang, Antarctic stratospheric chemistry of chlorine nitrate, hydrogen chloride, and ice: Release of active chlorine, *Science, 238,* 1253-1257, 1987.

Müller, R., T. Peter, P.J. Crutzen, H. Oelhaf, G.P. Adrian, T. von Clarmann, A. Wegner, U. Schmidt, and D. Lary, Chlorine chemistry and the potential for ozone depletion in the Arctic stratosphere in the winter of 1991/1992, *Geophys. Res. Lett., 21,* 1427-1430, 1994.

Müller, R., P.J. Crutzen, J.-U. Grooß,C. Brühl, J.M. Russel III, and A.F. Tuck, Chlorine activation and ozone depletion in the Arctic vortex: Observations by the Halogen Occultation Experiment on the Upper Atmosphere Research atellite, *J. Geophys. Res., 101,* 12531-12554, 1996.

Müller, R., P.J. Crutzen, J.-U. Grooß , C. Brül, J.M. Russell III, H. Gernandt, D.S. McKenna, and A.F. Tuck, Severe chemical ozone loss in the Arctic during the winter 1995-96. *Nature, 389,* 709-712, 1997.

Naujokat, B., and S. Pawson, The cold stratospheric winters 1994/95 and 1995/96, *Geophys. Res. Lett., 23* , 3703-3706, 1996.

Orlando, J.J., and J.B. Burkholder, Gas phase UV/visible absorption spectra of HOBr and Br_2O, *J. Geophys. Res. 99,* 1143, 1995.

Park, J.H., et al., Validation of Halogen Occultation Experiment CH_4 measurements from UARS, *J. Geophys. Res., 101,* 10183-10204, 1996.

Pierson, J.M., K.A. McKinney, D.W. Toohey, J.J. Margitan, U. Schmidt, A. Engel, and P.A. Newman, An investigation of ClO photochemistry in the chemically perturbed Arctic vortex, *J. Atmos. Chem., 32,* 61-81, 1999.

Proffitt, M.H., and R.J. McLaughlin, Fast-response dual-beam UV-absorption ozone photometer suitable for use on stratospheric balloons, *Rev. Sci. Instrum., 54,* 1719-1728, 1983.

Proffitt, M.H., J.J. Margitan, K.K. Kelly, M. Loewenstein, J.R. Podolske, and K.R. Chan, Ozone loss in the Arctic polar vortex inferred from high-altitude aircraft measurements, *Nature, 347,* 31-36, 1990.

Proffitt, M., S. Solomon, and M. Loewenstein, Comparison of 2-D model simulations of ozone and nitrous oxide at high latitudes with stratospheric measurements, *J. Geophys. Res., 97,* 939-944, 1992.

Proffitt, M.H., K. Aikin, J.J.Margitan, M. Loewenstein, J.R. Podolske, A. Weaver, K.R. Chan, H. Fast, and J.W. Elkins,

Ozone loss inside the northern polar vortex during the 1991/1992 winter, *Science, 261,* 1150-1154, 1993.

Pullen, S., and R.L. Jones, Accuracy of temperatures from the UKMO analyses of the 1994/95 in the Arctic winter stratosphere, *Geophys. Res. Lett., 24,* 845-848, 1997.

Rex, M., et al. , Chemical ozone loss in the Arctic winter 1994/95 as determined by the Match technique, *J. Atmos. Chem., 32,* 35-59, 1999.

Rinsland, C.P., et al., ATMOS measurements of $H_2O + 2CH_4$ and total reactive nitrogen in the November 1994 Antarctic stratosphere: Dehydration and denitrification in the vortex, *Geophys. Res. Lett., 23,* 2397-2401, 1996.

Salawitch, R.J., et al., Loss of ozone in the Arctic vortex for the winter of 1989, *Geophys. Res. Lett., 17,* 561-564, 1990.

Salawitch, R.J. et al., Chemical loss of ozone in the Arctic polar vortex in the winter of 1991-1992, *Science, 261,* 1146-1149, 1993.

Schmidt, U., G. Kulessa, E. Klein, E.-P. Röth, and R. Borchers, Intercomparison of balloon-borne cryogenic whole air samplers during the MAP/GLOBUS 1983 campaign, *Planet. Space Sci., 35,* 647-656, 1987.

Schmidt, U., R. Bauer, A. Engel, R. Borchers, and J. Lee, The variation of available chlorine Cly in the Arctic polar vortex during EASOE, *Geophys. Res. Lett., 21,* 1215-1218, 1994.

Solomon, S., Progress towards a quantitative understanding of Antarctic ozone depletion, *Nature, 347,* 347-354, 1990.

Sugita, T., Y. Kondo, H. Nakajima, U. Schnidt, A. Engel, H. Oelhaf, G. Wetzel, M. Koike, P.A. Newman, Denitrification observed inside the Arctic vortex in February 1995, *J. Geophys. Res., 103,* 16221-16233, 1998.

Toohey, D.W., L.M. Avallone, J.N. Demusz, N.L. Hazen, and J.G. Anderson, The performance of a new instrument for in situ measurements of ClO in the lower stratosphere, *Geophys. Res. Lett., 20,* 1791-1794, 1993.

von der Gathen, P., et al., Observational evidence for chemical ozone depletion over the Arctic in winter 1991-92, *Nature, 375,* 131-134, 1995.

Wamsley, P.R., et al., Distribution of halon-1211 in the upper troposphere and lower stratosphere and the 1994 total bromine budget, *J. Geophys. Res., 103,* 1513-1526, 1998.

Waters, J.W., L. Froidevaux, W.G. Read, G.L. Manney, L.S. Elson, D.A. Flower, R.F. Jarnot, and R.S. Harwood, Stratospheric ClO and ozone from the Microwave Limb Sounder on the Upper Atmosphere Research Satellite, *Nature, 362,* 597-602, 1993.

World Meteorological Organization, Scientific assessment of ozone depletion: 1994, *Rep. 37,* Geneva, 1994.

Zander, R., et al., The northern midlatitude budget of stratospheric chlorine derived from ATMOS/ATLAS 3 observations, *Geophys. Res. Lett., 23,* 2357-2361, 1996.

K.S. Carslaw, Environment Centre, University of Leeds, Leeds LS2 9JT, England, United Kingdom.

A. Engel, Institut für Meteorologie und Geophysik, J.W. Goethe Universität Frankfurt, 60325 Frankfurt, Germany.

J.J. Margitan and M. Rex, Jet Propulsion Laboratory, 4800 Oak Grove Drive, Pasadena, CA 91109.

D. McKenna, R. Müller, F. Stroh, and T. Woyke, Institut für Stratosphärische Chemie, Forschungszentrum Jülich, 52425 Jülich, Germany. (t.woyke@fz-juelich.de)

(Received December 3, 1998; revised March 12, 1999; accepted April 22, 1999.)